Influence of Secondary Interactions on the Structure, Sublimation Thermodynamics, and Solubility of Salicylate:4-Hydroxybenzamide Cocrystals. Combined Experimental and Theoretical...

ARTICLE *in* THE JOURNAL OF PHYSICAL CHEMISTRY B · AUGUST 2015

Impact Factor: 3.3 · DOI: 10.1021/acs.jpcb.5b05082 · Source: PubMed

6 AUTHORS, INCLUDING:

Alexey Manin

Institute of Solution Chemistry of RAS

22 PUBLICATIONS **100** CITATIONS

SEE PROFILE

Anastasia V. Shishkina

Mendeleev Russian University of Chemical T...

8 PUBLICATIONS **101** CITATIONS

SEE PROFILE

Mikhail V Vener

Mendeleev Russian University of Chemical T...

69 PUBLICATIONS **1,189** CITATIONS

SEE PROFILE

German L Perlovich

Institute of Solution Chemistry of RAS

142 PUBLICATIONS **1,479** CITATIONS

SEE PROFILE

THE JOURNAL OF PHYSICAL CHEMISTRY B

Article

pubs.acs.org/JPCB

Influence of Secondary Interactions on the Structure, Sublimation Thermodynamics, and Solubility of Salicylate:4-Hydroxybenzamide Cocrystals. Combined Experimental and Theoretical Study

Alex N. Manin,[†] Alexander P. Voronin,[†] Anastasia V. Shishkina,[‡] Mikhail V. Vener,[‡] Andrei V. Churakov,[§] and German L. Perlovich*[,†]

[†]G.A. Krestov Institute of Solution Chemistry, Russian Academy of Sciences, 1, Academicheskaya, 153045 Ivanovo, Russian Federation

[‡]Mendeleev University of Chemical Technology, 9, Miusskaya Square, 125047 Moscow, Russia

[§]Institute of General and Inorganic Chemistry, Russian Academy of Sciences, Leninskii Prosp. 31, 119991 Moscow, Russia

Supporting Information

ABSTRACT: Cocrystal screening of 4-hydroxybenzamide with a number of salicylates (salicylic acid, SA; 4-aminosalicylic acid, PASA; acetylsalicylic acid, ASA; and salicylsalicylic acid, SSA) was conducted to confirm the formation of two cocrystals, [SA +4-OHBZA] (1:1) and [PASA+4-OHBZA] (1:1). Their structures were determined using single-crystal X-ray diffraction, and the hydrogen-bond network topology was studied. Thermodynamic characteristics of salicylic acid cocrystal sublimation were obtained experimentally. It was proved that PASA cocrystallization with 4-OHBZA makes the drug more stable and prevents the irreversible process of decarboxylation of PASA resulting in formation of toxic 3-aminophenol. The pattern of non-covalent interactions in the cocrystals is described quantitatively using solid-state density functional theory followed by Bader analysis of the periodic electron density. It has been found that the total energy of secondary interactions between synthon atoms and the side hydroxyl group of the acid molecule in [SA+4-OHBZA] (1:1) and [PASA+4-OHBZA] (1:1) cocrystals is comparable to the energy of the primary acid−amide heterosynthon. The theoretical value of the sublimation enthalpy of [SA+4-OHBZA], 231 kJ/mol, agrees fairly well with the experimental one, 272 kJ/mol. The dissolution experiments with [SA+4-OHBZA] have proved that the relatively large cocrystal stability in relation to the stability of its components has a negative effect on the dissolution rate and equilibrium solubility. The [PASA+4-OHBZA] (1:1) cocrystal showed an enhancement of apparent solubility compared to that of the corresponding pure active pharmaceutical ingredient, while their intrinsic dissolution rates are comparable.

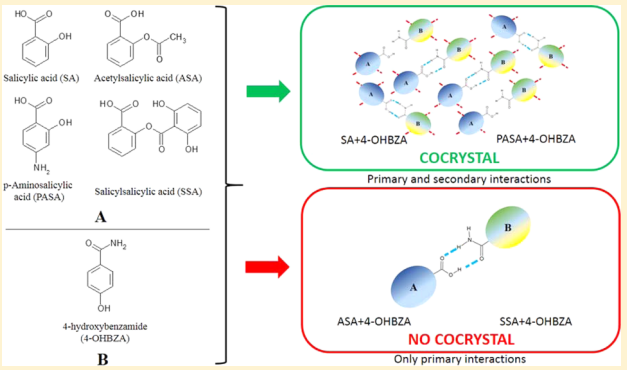

1. INTRODUCTION

One of the most effective approaches to improving physicochemical properties of active pharmaceutical ingredients (APIs) is pharmaceutical cocrystallization.[1−3] A strength of cocrystal formation is the essential improvement of the dissolution profile of target APIs without affecting their molecular structure and biological activity, along with high product stability. Additional valuable advantages of cocrystal formation for the pharmaceutical industry include the possibility of extending the life cycles of old APIs and protecting intellectual property.[4] However, the outcome of cocrystallization processes cannot yet be reliably predicted, along with the physicochemical properties of the resulting solid. This leads researchers to discover new cocrystalline forms based on semiempirical approaches and various screening algorithms.[5]

The key to the understanding of the formation of cocrystals lies in the concept of supramolecular synthons.[6] Recently, a concept of primary and secondary interactions was introduced to describe the process of cocrystal formation. The primary interactions give robust synthons, and the secondary interactions are all other weaker intermolecular contacts.[7] It should be noted that the focus of investigations in published articles has been on primary heterosynthons formation and intermolecular interactions, forming infinite chains of homo- and heterodimers in crystals.[8,9] At the same time, it was proved that a high possibility of primary heterosynthons formation does not always guarantee that cocrystals will be obtained.[10] Much less

Received: May 28, 2015
Revised: July 28, 2015

DOI: 10.1021/acs.jpcb.5b05082
J. Phys. Chem. B XXXX, XXX, XXX−XXX

attention has been paid to the systematic study of secondary interactions in the cocrystal.[11,12]

Here, the following salicylates were chosen as the cocrystal APIs: salicylic acid (SA), acetylsalicylic acid (or aspirin, ASA), para-aminosalicylic acid (PASA), and salicylsalicylic acid (or salsalate, SSA) (Chart 1). 4-Hydroxybenzamide (4-OHBZA)

Chart 1. Molecular Structure of Salicylates and 4-Hydroxybenzamide

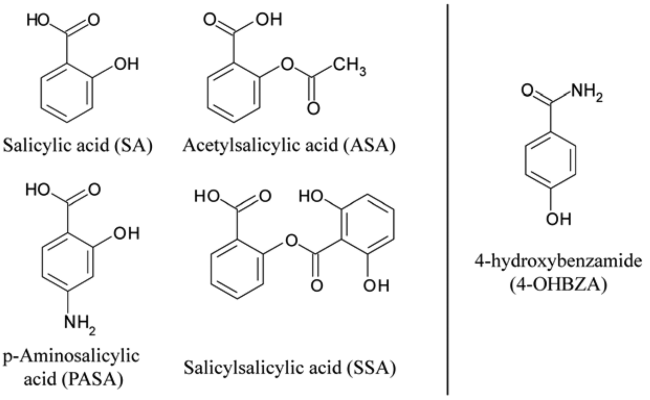

was taken as the cocrystal former, as it contains a carboxamide functional group capable of forming strong hydrogen bonds with carboxylic acids.[13] Some benzoic acid and benzamide derivatives had already been used as possible coformers in our previous paper examining the features of several experimental cocrystal screening methods.[14] In particular, it was established that 4-OHBZA forms a stable cocrystal with salicylic acid. In the present work, we have extended the group of salicylates to four.

Notwithstanding their related structures, the pharmaceutical and physicochemical properties of salicylates are significantly different. According to the Biopharmaceutics Classification System (BCS), salicylates belong to different classes of drugs. SA and ASA, with high solubility and permeability, belong to class I.[15,16] PASA is located on the boundary between classes II and IV, with low solubility and permeability about 80%.[16] There is no information about SSA in the open sources.

Salicylates are non-steroidal anti-inflammatory drugs, which are actively used in medicine. Salicylic acid is used as a constituent of some rubefacient products. Salicylic acid and aspirin are applied in medicine as anti-pyretic, anti-inflammatory, anti-rheumatic, and analgesic drugs.[17] Para-aminosalicylic acid is well-known as an anti-tubercular drug.[18] Salicylsalicylic acid is used for the treatment of diabetes.[15] Salicylates are used not only as APIs but also as cocrystal formers.[18−23] The most popular coformer is salicylic acid, with 40 cocrystals (see Supporting Information, "Database Studies for Acids").

Our research work is devoted to the experimental and theoretical study of structural and thermodynamic aspects of salicylates with 4-OHBZA cocrystallization and investigation of the cocrystal structures' influence on dissolution properties. The presence of acid and amide functional groups in the crystal structures of the chosen coformers suggests that cocrystallization has to go through acid−amide heterosynthon formation of complexes with 1:1 stoichiometry. The suggestion was confirmed by analysis of the Crystal Structure Database (CSD) and literature data (see Supporting Information, "Results of the CSD Analysis"). Gas-phase computations of salicylate:4-OHBZA heterodimers have shown that the energy of the acid−amide heterosynthon is virtually the same for all four systems of the systems studied (Table S1), so the probability of cocrystallization is assumed to be equally high. However, the experimental screening has proved the formation of only two cocrystals: those with salicylic and para-aminosalicylic acids (Table S2, Figures S1−S4). The single crystals were grown and the crystal structures solved in order to discuss the packing features of new cocrystals. The cocrystal stability can be measured by crystal lattice energy that is usually obtained from sublimation enthalpy in the sublimation experiment. The experimental measurement of cocrystal sublimation thermodynamics was conducted by the transpiration method, as described in our previous work.[24] Solid-state DFT calculations followed by Bader analysis of the periodic electron density were performed to evaluate the energy contributions of acid−amide synthon and secondary interactions to the crystal lattice energy. As sublimation enthalpy of a solid determines its solubility characteristics, the dissolution study was performed for the obtained cocrystals.

2. MATERIALS AND METHODS

2.1. Compounds and Solvents. Salicylic acid ($C_7H_6O_3$, MW 138.121, purity ≥99.5%), acetylsalicylic acid ($C_9H_8O_4$, MW 180.157, purity 99%), para-aminosalicylic acid ($C_7H_7NO_3$, MW 153.135, purity 99%), salicylsalicylic acid ($C_{14}H_{10}O_5$, MW 258.23, purity ≥98%), and 4-hydroxybenzamide ($C_7H_7NO_2$, MW 137.14, purity 98%) were purchased from Sigma-Aldrich. All solvents were of analytical grade and used as received without further purification.

2.2. Grinding Experiment. Solvent-drop grinding experiments were performed using a Fritsch planetary micro mill, model Pulverisette 7, in 12 mL agate grinding jars with a total of 10, 5 mm agate balls at a rate of 600 rpm for 60 min. The experiments were carried out with stoichiometric amounts of salicylates and 4-hydroxybenzamide and a few drops of solvent (methanol or ethanol) added by a micropipet.

2.3. Differential Scanning Calorimetry (DSC). Thermal analysis was carried out using a DSC 204 F1 Phoenix differential scanning heat flux calorimeter (NETZSCH, Germany) with a high-sensitivity μ-sensor. The sample was heated at the rate of 10 K·min^{-1} in an Ar atmosphere and cooled with liquid N_2. Temperature calibration of the DSC was performed against six high-purity substances: cyclohexane (99.96%), mercury (99.99+%), biphenyl (99.5%), indium (99.999%), tin (99.999%), and bismuth (99.9995%). The accuracy of the weighing procedure was ±0.01 mg.

2.4. Crystallization Procedure. *[SA+4-OHBZA] (1:1).* Equimolar amounts of salicylic acid and 4-hydroxybenzamide were dissolved in ethanol and stirred at room temperature. The resulting clear solution was filtered and allowed to evaporate. Diffraction quality crystals were grown over 3 days.

[PASA+4-OHBZA] (1:1). Para-aminosalicylic acid and 4-hydroxybenzamide in a 1:1 molar ratio were ground with ethanol for half an hour and then dissolved in acetone and stirred at room temperature. The resulting clear solution was filtered, covered by parafilm perforated with a few small holes, and allowed to evaporate slowly. Diffraction-quality crystals were grown over a few days.

2.5. Single-Crystal X-ray Diffraction. X-ray reflections were collected on a Bruker-Nonius X8-APEXII CCD diffractometer using graphite-monochromated Mo Kα radiation (λ = 0.7107 Å) at 150 K. Powder X-ray diffraction data were recorded under ambient conditions in Bragg−Brentano

DOI: 10.1021/acs.jpcb.5b05082
J. Phys. Chem. B XXXX, XXX, XXX−XXX

geometry with a Bruker D8 Advance diffractometer with Cu Kα radiation (λ = 1.5406 Å).

2.6. Powder X-ray Diffraction (PXRD). The powder materials of the grinding experiments were identified by using a D8 Advanced powder X-ray diffractometer (Bruker AXS GmbH, Germany), with Mo Kα radiation. The voltage and current applied were 40 kV and 40 mA, respectively. The data were collected in the range of 2θ = 5−30°, with a step size 0.03°.

2.7. Sublimation Measurements. Sublimation experiments were carried out by the transpiration method as described elsewhere.[25,26] In brief, a stream of an inert gas passes above the sample at a constant temperature and at a known slow constant flow rate in order to achieve saturation of the carrier gas with the vapor of the substance under investigation. The vapor is condensed at some point downstream, and the mass of sublimate and its purity are determined by UV−vis spectrophotometry and DSC. The vapor pressure over the sample at this temperature can be calculated on the basis of the amount of the sublimated sample and the volume of the inert gas used.

2.8. Solubility and Dissolution Experiments. Dissolution measurements were carried out by the shake-flask method at 25.0 ± 0.1 °C. The samples were suspended in 10 mL of pH 7.4 phosphate buffer in Pyrex glass tubes. The amount of SA or PASA and the cocrystals dissolved was measured by taking 1 mL aliquots of the respective media. The solid phase was removed by isothermal filtration (Rotilabo syringe filter, PTFE, 0.2 μm), and the concentration was determined by high-performance liquid chromatography (HPLC). The results are stated as the average of at least three replicated experiments. HPLC was performed on Shimadzu Prominence model LC-20AD instrument equipped with a PDA detector and a C-18 column (150 mm × 4.6 mm i.d., 5 μm particle size, and 100 Å pore size).

Intrinsic dissolution rate (IDR) measurements were carried on a USP-certified Electrolab EDT-08LX dissolution tester by the disk intrinsic dissolution method. For IDR experiments, approximately 200 mg of pure SA or PASA and the cocrystals were compressed by a hydraulic press for 5 min to form a nonporous compact of 8 mm diameter. The intrinsic attachment with the sample was rotated at 120 rpm in 500 mL of pH 7.4 phosphate buffer, preheated to 37.0 °C. The cumulative amount dissolved per unit surface area was determined by taking 1 mL aliquots of the respective media every 5−6 min, with the volume replacement and concentration measured by HPLC. The slope of the plot of mass dissolved per unit surface area vs time gives the IDR in appropriate units, e.g., mg min^{-1} cm^{-2}.

The samples were eluted with a mobile phase with different compositions. Compositions of the mobile phases and retention times for the coformers in the cocrystal and pure components are presented in Table S3. Phosphate buffer, pH 3.5, was prepared from KH_2PO_4 (0.05 M concentration) and H_3PO_4 (85% m.f.) Peak areas obtained from the HPLC analysis were plotted against the concentration to obtain the calibration plot. Solution concentrations were calculated from the respective calibration plot of the coformers and cocrystals. All of the samples remaining after the dissolution experiments were analyzed by DSC or PXRD, and it was found that the cocrystal integrity was not intact after the dissolution experiment.

3. CALCULATION PROCEDURE

Density functional theory computations with periodic boundary conditions (solid-state DFT) were performed in the Crystal14[27] software package using B3LYP and PBE functionals in localized basis sets 6-31G** and pob-TZVP,[28] respectively. The B3LYP/6-31G** approximation provides reliable and consistent results in studying the intermolecular interactions in crystals.[29] PBE is widely employed in theoretical studies of H-bonded systems in the crystalline state.[30] For [PASA+4-OHBZA] (1:1) cocrystal a calculation with empirical Grimme correction D2 was performed.[31] Details of solid-state DFT calculations are given in SI. Bader analysis of periodic electron density[32,33] was performed in TOPOND14[34] The following electron-density features at the bond critical point were computed: (i) the values of the electron density, ρ_b; (ii) the Laplacian of the electron density, $\nabla^2\rho_b$; and (iii) the positively defined local electronic kinetic energy density, G_b. Non-covalent (intermolecular) interactions with ρ_b < 0003 a.u. were not considered in present work, as their value is too small for determination by existing experimental and computational methods.[35,36] The energy of the particular single non-covalent interaction, E_{int}, was estimated as[37]

$$E_{int} = 0.429G_b \quad \text{(in atomic units)} \tag{1}$$

Eq 1 yields reasonable E_{int} values for molecular crystals with H-bonds, C−H···O and π-stacking contacts, etc.[36,38,39]

There are several theoretical approaches to assessing lattice energy E_{latt} in crystalline materials; see, e.g., refs 41 and 42. In our paper, we use the approach proposed in ref 43. It views the lattice energy as a sum of the energies of non-covalent interactions between the considered molecule (heterodimer) and its neighbors:

$$E_{latt} = \sum_i \sum_{j<i} E_{int,j,i} \tag{2}$$

where $E_{int,j,i}$ is the energy of a particular non-covalent interaction. Indices j and i denote the atoms belonging to different molecules. E_{int} can be evaluated using the pairwise potentials (Gavezzotti approach)[44,45] or from eq 1. The latter approach provides reasonable values for single-component[37,40] and two-component[24,46] molecular crystals. If the interaction energies are obtained using the $E_{int} - G_b$ scheme, eq 2 is free of the basis set superposition error.

It is assumed that the E_{latt} energy corresponds to the sublimation enthalpy ΔH^0_{subl}, extrapolated to 0 K. According to ref 47, the value of the sublimation enthalpy at given temperature T can be written as

$$\Delta H_{sub}(\text{theor}) = -E_{latt} - 2RT \tag{3}$$

Details of gas-phase DFT calculations are given in the Supporting Information.

4. RESULTS AND DISCUSSION

As mentioned above, despite the evident structural significance of the formation of heterosynthon in cocrystals, studies of the other types of intermolecular hydrogen bonds are rarely conducted. However, our CSD search of cocrystals with the objects of our investigation shows that in addition to the primary acid−amide heterosynthon, cocrystallization produced more than 10 different types of hydrogen bonds between coformer molecules. For several cocrystals they are primary heterosynthons (for example, O−H(carboxyl)···N(pyridine)

DOI: 10.1021/acs.jpcb.5b05082
J. Phys. Chem. B XXXX, XXX, XXX−XXX

hydrogen bonds in cocrystals with pyridine derivatives[9,22,23]), but otherwise, secondary interactions play an important role in cocrystal formation (see Supporting Information, "Results of the CSD Analysis"). The analysis of hydrogen bond network topology has proved the role of secondary interactions involving the side functional groups of both acid and 4-OHBZA molecules.

4.1. Crystal Structure Analysis. The structures of [SA+4-OHBZA] (1:1) and [PASA+4-OHBZA] (1:1) were determined by single-crystal X-ray diffraction (Table 1). [SA+4-OHBZA] (1:1) crystallizes from ethanol in the monoclinic $P2_1/c$ space group. [PASA+4-OHBZA] (1:1) was obtained from acetone. It belongs to the orthorhombic $Pca2_1$ space group (Table 1). The asymmetric unit in both cocrystals consists of 1:1 [A+B] heterodimer. It is stabilized by the acid···amide synthon in a $R_2^2(8)$ motif (Figure 1a). The O1···O4 and N1···O2 distances in heterodimers are rather short, ∼2.6 and ∼2.9 Å, respectively (Table 2). The intermolecular N−H···O and O−H···O bonds are generally linear, in the range from 164 to 176°.

Table 1. Crystal Lattice Parameters of [SA+4-OHBZA] and [PASA+4-OHBZA]

	[SA+4-OHBZA] (1:1)	[PASA+4-OHBZA] (1:1)
CCDC code	1403606	1403605
crystal system	monoclinic	orthorhombic
space group	$P2_1/c$	$Pca2_1$
crystal size, mm	0.35 × 0.30 × 0.30	0.20 × 0.20 × 0.15
a, Å	13.8869(5)	32.1000(15)
b, Å	8.01874(18)	4.1188(2)
c, Å	12.8184(4)	9.6966(4)
α, °	90.00	90.00
β, °	115.187(4)	90.00
γ, °	90.00	90.00
volume, Å^3	1291.69	1282.02
Z	4	4
D_{calc}, g·cm^{-3}	1.415	1.504
radiation	Mo Kα	Mo Kα
T, K	423(10)	120(2)
μ, mm^{-1}	0.109	0.116
	Data Collection	
measd reflns	3163	5183
indep reflns	3108	1968
indep reflns >2$\sigma(I)$	2432	1857
R_{int}	0.0295	0.0254
θ_{max}, °	29.34	29.984
	Refinement	
refinement on	F^2	F^2
$R[F^2 > 2\sigma(F^2)]$	0.0391	0.356
$\omega R(F^2)$	0.0920	0.0884
S	1.038	1.030
reflections	3108	1968
parameters	233	246
$(\Delta/\sigma)_{max}$	<0.001	0.000
$\Delta\rho_{max}$, e·Å^{-3}	0.250	0.358
$\Delta\rho_{min}$, e·Å^{-3}	−0.206	−0.165

Heterodimer packing of cocrystals [SA + 4-OHBZA] (1:1) is similar to the molecular packing in the [salicylamide+4-hydroxybenzoic acid] cocrystal.[48] The spatial arrangement of the molecules in these cocrystals is almost identical (Figure S5). Side functional groups of SA and 4-OHBZA molecules play an essential role in the packing of the heterodimers in the cocrystal. The "tail" hydroxyl group of 4-OHBZA forms a moderate O5−H5a···O4 bond, R(O···O) ≈ 2.69 Å, with the oxygen atom of the carbonyl group of the adjacent benzamide molecule (Table 2). The NH_2 group of 4-OHBZA forms an N1−H1b···O3 bond of moderate strength, R(N···O) ≈ 2.98 Å, with the OH-group of the adjacent molecule of salicylic acid (Table 2). By these two H-bonds (Figure 1) the [SA+4-OHBZA] heterodimers assemble into twin infinite 3D networks in $R_6^6(30)$ secondary motif (Figure 1b, color shows molecules with different orientation in a single network). The adjacent homodimers are arranged at an angle of ∼60° to each other due to steric hindrance (Figure 1c). The networks (Figure 1c, shown green and yellow) interact with each other in a crystal through weaker C−H···O contacts and π-stacking interactions (Table S4 and subsection 4.3).

The crystal packing in [PASA+4-OHBZA] (1:1) is given in Figure 2. It differs greatly from that of [SA+4-OHBZA] (1:1), cf. Figures 1c and 2b, due to the presence of an NH_2 group in the PASA molecule. Specifically, the nitrogen atom N2 forms a relatively strong H-bond with the side OH group of 4-OHBZA, R(N···O) ≈ 2.73 Å, Table 2. It assembles heterodimers in chains (see Figure 2a). The "secondary" tail-to-side O5−H5a···O4 interaction in [SA+4-OHBZA] (1:1) is replaced by a much stronger "tail-to-tail" O5−H5a···N2 interaction in [PASA+4-OHBZA] (1:1). This causes a nearly parallel arrangement of molecules in the [PASA+4-OHBZA] (1:1) cocrystal (Figure 2b). N1−H1b···O4 side hydrogen bonds, R(N···O) ≈ 3.22 Å, connect 4-OHBZA molecules of the proximate parallel oppositely faced chains into infinite C(4) motifs analogous to those in a crystal of pure 4-OHBZA. Side OH groups of PASA and 4-OHBZA accept weak H-bonds from the NH_2 group of PASA (R(N···O) > 3 Å) and thus stabilize the neighboring chains (Table S5 and subsection 4.3).

4.2. Thermodynamic Characteristics of Cocrystal Sublimation. Thermodynamic conditions of molecules in solids can be described by sublimation characteristics. Moreover, comparison of thermodynamic parameters of sublimation process of the cocrystal and its coformers may help us understand energetic aspects of cocrystal formation. In our previous work, we measured the cocrystal sublimation parameters by the transpiration method and proposed a presumable mechanism of the sublimation process.[24]

[SA+4-OHBZA] (1:1). Figure 3 represents temperature dependences of vapor pressure for cocrystal and its components. Individual components were studied by us earlier.[49,50] The sublimation thermodynamic parameters of the cocrystal and its conformers are presented in Table 3.

The sublimation experiment has shown that there is only salicylic acid in the condensed phase (Figure S6). Therefore, we deduced that the cocrystal falls into parts during sublimation, and 4-OHBZA precipitates from the supersaturation state in the oven. Cocrystal decomposition goes on without chemical transformations, with all intermolecular interactions being destructed. Therefore, we have obtained the value of the crystal lattice energy numerically equal to the dissociation energy of all the intermolecular interactions.[24]

The Gibbs energy of cocrystal sublimation process is numerically close to the Gibbs energy of 4-OHBZA sublimation process (Table 3). It is interesting to note that the enthalpy term of Gibbs energy of cocrystal sublimation

DOI: 10.1021/acs.jpcb.5b05082
J. Phys. Chem. B XXXX, XXX, XXX−XXX

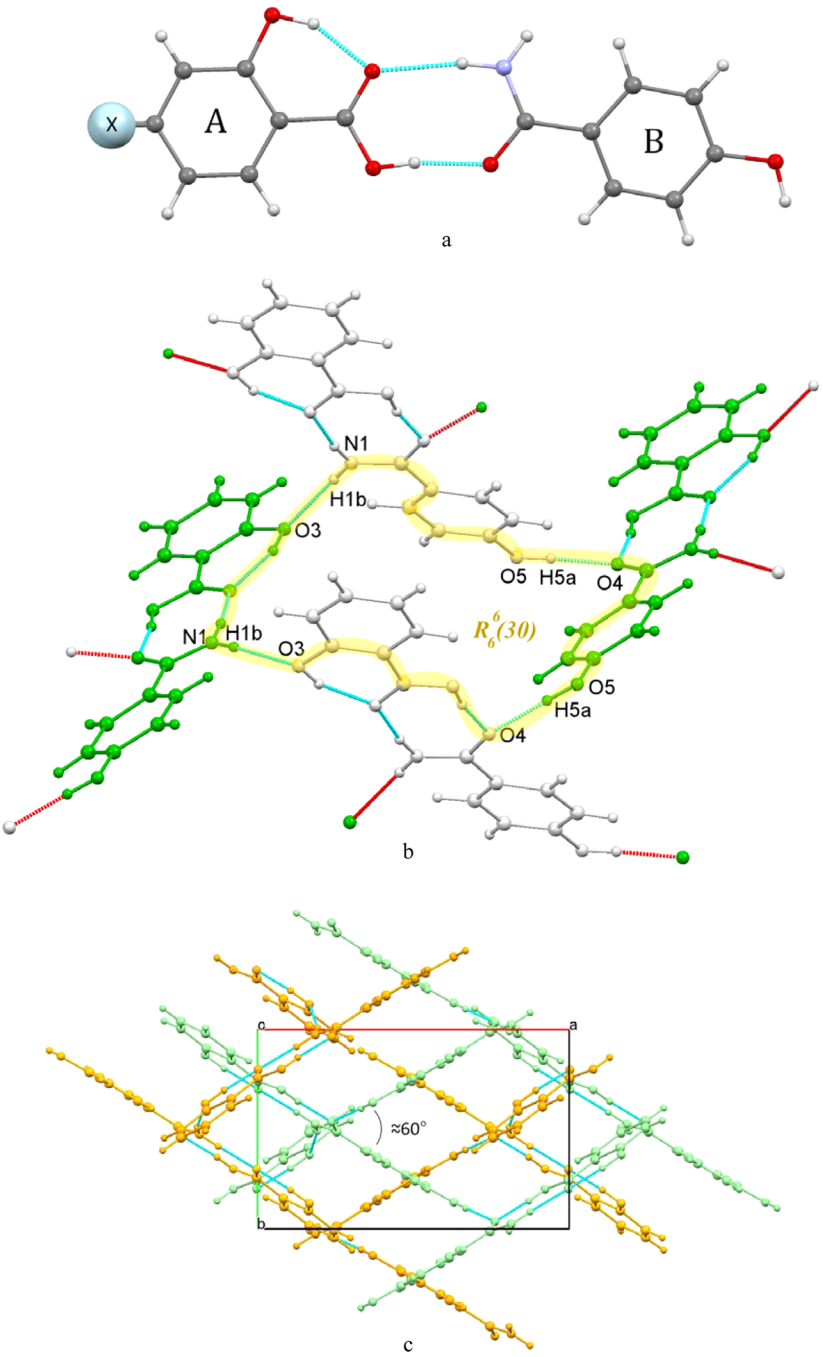

Figure 1. Acid−amide heterosynthon (X = H, NH_2) (a), the supramolecular unit of the infinite 3D network (b), and packing of the twin networks (c) in the [SA+4-OHBZA] cocrystal.

process has greatly increased compared to the terms of individual components. Despite the fact that the biggest contribution to cocrystal stabilization is made by the enthalpy term of Gibbs energy, the entropy term has a significant influence too. The entropy term growth may be explained by the increase in the free volume for molecules of coformers in the cocrystal.

The experimental value of [SA+4-OHBZA] (1:1) cocrystal sublimation enthalpy is 272 ± 8 kJ/mol, significantly higher than the sum of sublimation enthalpies of the coformers in pure forms (Table 3). We obtained contrary results in our previous work.[24] Crystal lattice energy of 2-hydroxybenzamide cocrystal was lower than the sum of the coformers enthalpy sublimation. This divergence can be explained by the features of hydrogen bond networks. The quantities of donors and acceptors of hydrogen bonds in [SA+4-OHBZA] (1:1) cocrystal are equal to each other, whereas the number of hydrogen bond donors for 2-hydroxybenzamide cocrystal is bigger than that of acceptors. Thus, the formation of bifurcational (polycenter) hydrogen bonds is quite likely for 2-hydroxybenzamide cocrystal, with their energy being significantly lower than that of hydrogen bonds with one center.

The numbers of hydrogen bond donors and acceptors in crystals of pure components of [SA+4-OHBZA] (1:1) are also different, which leads to weaker polycenter bonds in 4-OHBZA and acceptors not involved into crystal building in SA.

DOI: 10.1021/acs.jpcb.5b05082
J. Phys. Chem. B XXXX, XXX, XXX−XXX

Table 2. Experimental Values of the D−H and D···A Distances and Angles D−H···A of the D−H···A Unit, Where D = O or N, in the Considered Cocrystals

D−H···A[a]	symmetry code	D−H, Å	D···A, Å	D−H···A, °
		[SA+4-OHBZA] (1:1)		
O1−H1···O4	(*x*,*y*,*z*)	0.926	2.606	170.1
N1−H1a···O2	(*x*,*y*,*z*)	0.933	2.925	168.5
N1−H1b···O3	$(-x,{}^{1}/_{2}+y,{}^{1}/_{2}-z)$	0.894	2.979	163.6
O5−H5a···O4	$(1-x,{}^{1}/_{2}+y,{}^{1}/_{2}-z)$	0.929	2.687	167.0
O3−H3a···O2[b]	(*x*,*y*,*z*)	0.939	2.568	152.4
		[PASA+4-OHBZA] (1:1)		
O1−H1···O4	(*x*,*y*,*z*)	0.856	2.571	164.1
N1−H1a···O2	(*x*,*y*,*z*)	0.916	2.917	164.5
N1−H1b···O4	$(1-x,2-y,{}^{1}/_{2}+z)$	0.827	3.221	166.8
N2−H2a···O5	$(-{}^{1}/_{2}+x,2-y,z)$	0.879	3.069	159.7
N2−H2a···O3	$({}^{1}/_{2}-x,y,-{}^{1}/_{2}+z)$	0.879	3.109	115.8
N2−H2b···O3	$({}^{1}/_{2}-x,y,-{}^{1}/_{2}+z)$	0.876	3.167	126.2
O5−H5a···N2	$(-{}^{1}/_{2}+x,1-y,z)$	0.809	2.731	173.8
O3−H3a···O2[b]	(*x*,*y*,*z*)	0.872	2.573	154.0

[a]See Figures 2 and 4. [b]Intramolecular hydrogen bond.

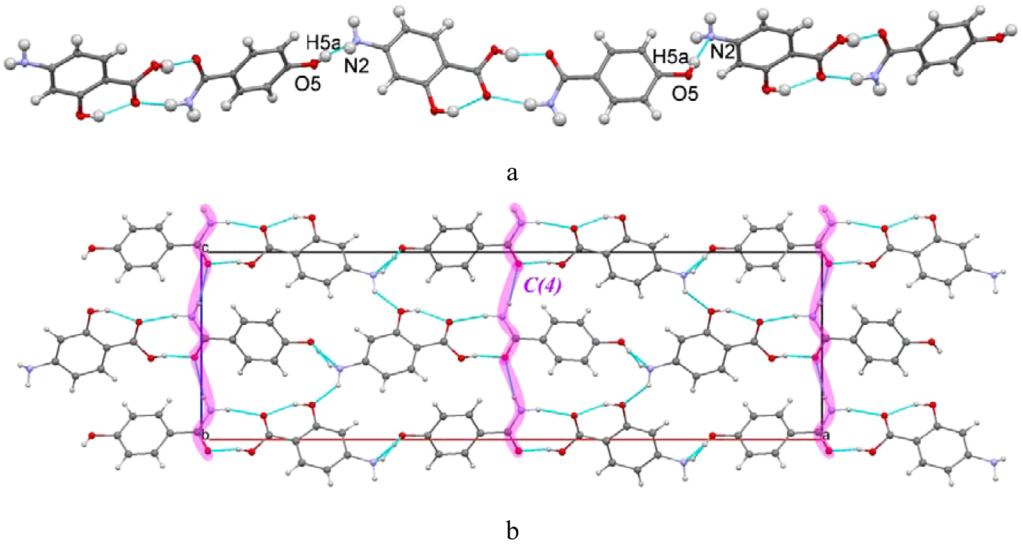

Figure 2. Infinite chains of heterodimers (a) and crystal packing (b) in the [PASA+4-OHBZA] (1:1) cocrystal.

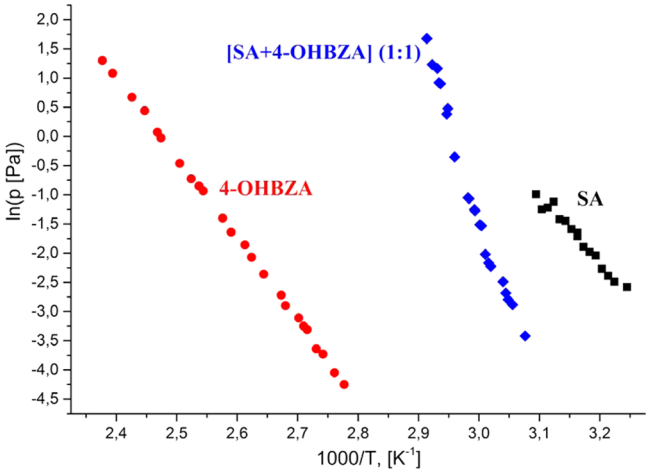

Figure 3. Temperature dependences of vapor pressure of the cocrystal and its components in pure form.

Table 3. Thermodynamic Parameters of Sublimation Processes of Cocrystal Components: Salicylic Acid (SA) and 4-Hydroxybenzamide (4-OHBZA)[a]

	[SA+4-OHBZA] (1:1)	SA[49]	4-OHBZA[50]
ΔG^{298}_{sub}, kJ·mol^{-1}	60.6	38.5	58.9
ΔH^{T}_{sub}, kJ·mol^{-1}	272 ± 8	95.5 ± 0.8	115.6 ± 0.6
ΔH^{298}_{sub},[b] kJ·mol^{-1}	273 ± 8	96.6 ± 0.8	117.8 ± 0.6
$T\Delta S^{298}_{sub}$, kJ·mol^{-1}	213	56.9	58.9
ΔS^{298}_{sub}, J·mol^{-1}·K^{-1}	714 ± 30	191 ± 3	198 ± 2
T_m, K	448 ± 0.2	431.2 ± 0.2	433 ± 0.2
$C^{298}_{p,cr}$,[c] J·mol^{-1}·K^{-1}	285 ± 1	133 ± 1	152 ± 1
ς_H,[d] %	56.2	63.4	66.7
ς_{TS},[e] %	43.8	36.6	33.3

[a]$\ln(P\ (\mathrm{Pa})) = (96.84 \pm 2.95) - (32729 \pm 990)/T$; $R = 0.9901$; $\sigma = 5.18 \times 10^{-2}$; $n = 23$. [b]$\Delta H^{298}_{sub} = \Delta H^{T}_{sub} + [0.75 + 0.15C^{298}_{p,cr}(298.15)](T - 298.15)$. [c]Calculated by Chickos's additive scheme.[51] [d]$\varsigma_H = [\Delta H^{0,298}_{sub}/(\Delta H^{0,298}_{sub} + T\Delta S^{298}_{sub})] \times 100\%$. [e]$\varsigma_{TS} = [T\Delta S^{298}_{sub}/(\Delta H^{0,298}_{sub} + T\Delta S^{0,298}_{sub})] \times 100\%$.

DOI: 10.1021/acs.jpcb.5b05082
J. Phys. Chem. B XXXX, XXX, XXX−XXX

Therefore, the ΔH^{298}_{sub} value of [SA+4-OHBZA] (1:1) is expected to be larger than the sum of the ΔH^{298}_{sub} values of crystalline 4-OHBZA and SA.

[PASA+4-OHBZA] (1:1). It is known that PASA is an unstable compound, which is inclined to irreversible decarboxylation with formation of 3-aminophenol in acid medium.[52] The sublimation experiment of PASA at 50 °C for a few hours gave a sufficient amount of sublimated compound for UV spectrophotometry analysis. The analysis showed a single 3-aminophenol peak at 285 nm[53] (Figure 4). It means that experimental studies of sublimation processes in PASA and its cocrystal are impossible.

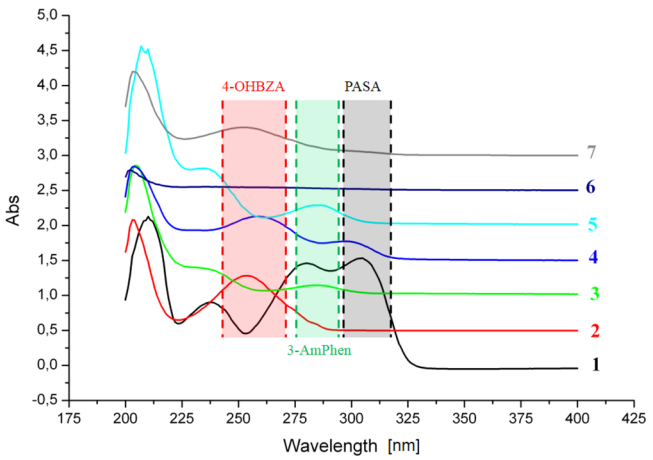

Figure 4. UV spectra for PASA (1), 4-OHBZA (2), 3-aminophenol (3), [PASA+4-OHBZA] (1:1) (4), sublimated sample of PASA (t_{exp} = 50 °C) (5), sublimated sample of [PASA+4-OHBZA] (1:1) (t_{exp} = 50 °C) (6), and sublimated sample of [PASA+4-OHBZA] (1:1) (t_{exp} = 90 °C) (7).

However, the experiment with the [PASA+4-OHBZA] (1:1) cocrystal shows changes in the PASA sublimation process. The sublimation experiment of the cocrystal with the same temperature and within the same time interval did not allow us to obtain a sufficient amount of the sublimated compound for UV analysis (Figure 4). It was only obtained at t = 90 °C. The comparison of UV profiles shows that the sublimated substance is 4-OHBZA; the typical peaks for PASA and 3-aminophenol are not observed. As PASA molecules were found to decompose upon sublimation, the lattice energy was estimated only theoretically.

4.3. Pattern of Non-covalent Interactions and the Lattice Energy. Solid-state DFT computations followed by Bader analysis of the periodic electronic density enables us to detect and quantify the pattern of non-covalent interactions in the cocrystals as well as to assess the cocrystal stability by calculating its lattice energy.

Theoretical values of the electron density parameters in the H···O bond critical point of the selected intermolecular H-bonds in [SA+4-OHBZA] (1:1) are given in Table 4. Most of the intermolecular (non-covalent) interactions in the crystal are characterized by $\nabla^2\rho_b > 0$ and $\rho_b < 0.03$ a.u. and, therefore, correspond to the case of the closed-shell interactions.[54] $\rho_b >$ 0.06 au for the synthon O−H···O bond indicates that it corresponds to an intermediate (transit) region, separating the shared (covalent) and closed-shell (non-covalent) interactions.[55,56] This H-bond is the strongest one in the cocrystal, $E_{int} \approx 55$ kJ/mol. The energy of the synthon N−H···O bond is around 21 kJ/mol. The theoretical energy of the acid···amide synthon is equal 76 kJ/mol (Table 4), in accordance with the available data.[7,10,42] A large number of relatively weak ($E_{int} < 10$ kJ/mol) intermolecular (non-covalent) interactions in the cocrystal are also quantifed. The obtained results are collected in Table S4. (It should be noted that the existence of short intermolecular contact does not imply the existence of the intermolecular interaction.[57]) All oxygen atoms of salicylic acid and benzamide molecules are involved in the formation of the C−H···O contacts (Figures 5, S7, and S8). Their energy varies from ∼5 to 10 kJ/mol (Table S4). A lot of C−H groups are involved in the formation of non-covalent interactions of different types. Their energy is relatively small, about 4 kJ/mol (Table S4).

Theoretical values of the electron density parameters in the H···O bond critical point of the selected intermolecular H-bonds of [PASA+4-OHBZA] (1:1) are given in Table 5. The acid−amide synthon energy equals ∼83 kJ/mol. It is 7 kJ/mol higher than that in the [SA+4-OHBZA] cocrystal, cf. Tables 4 and 5. Such difference is caused by the relatively short O1−H1···O4 distance in [PASA+4-OHBZA] dimer in comparison with that in [SA+4-OHBZA] (Table 2). All oxygen atoms of PASA and 4-OHBZA are involved in the formation of C−H···

Table 4. Theoretical Values[a] of the D···O and H···O Distances, R(D···O) and R(H···O), of the D—H···O Fragments (Where D = O, N, or C) and Electron Density Properties in the H···O Bond Critical Point of the Selected Intermolecular H-Bonds of [SA +4-OHBZA] (1:1)

interaction	fragment	R(D···O), Å (R(H···O), Å)	ρ_b, a.u.	$\nabla^2\rho_b$, a.u.	G_b, a.u.	E_{int},[b] kJ·mol^{-1}
		Synthon Interactions[c]				
A···B	O1−H1···O4	2.554 (1.548)	0.065	0.166	0.049	55.3
	N1−H1a···O2	2.954 (1.951)	0.026	0.072	0.019	21.1
					Total:	***76.4***
		Side Interactions of the Synthon Atoms and O3H3a Group[c]				
B···B′	O4···H5a−O5	2.673 (1.692)	0.044	0.137	0.034	38.0
B···A′	N1−H1b···O3	2.984 (1.978)	0.023	0.067	0.017	19.6
B···A′	C13−H13···O3	3.372 (2.436)	0.011	0.035	0.008	9.1
A···A′	O1···H5−C5[d]	3.540 (2.515)	0.008	0.027	0.006	6.8
A···A′	O2···H6−C6[e]	3.422 (2.669)	0.006	0.024	0.005	5.4
					Total:	***78.9***

[a]Evaluated by solid-state B3LYP/6-31G** followed by Bader analysis of the periodic electronic density. [b]Eq 1. [c]See Figure 5. [d]See Figure S8. [e]See Figure S7.

DOI: 10.1021/acs.jpcb.5b05082
J. Phys. Chem. B XXXX, XXX, XXX−XXX

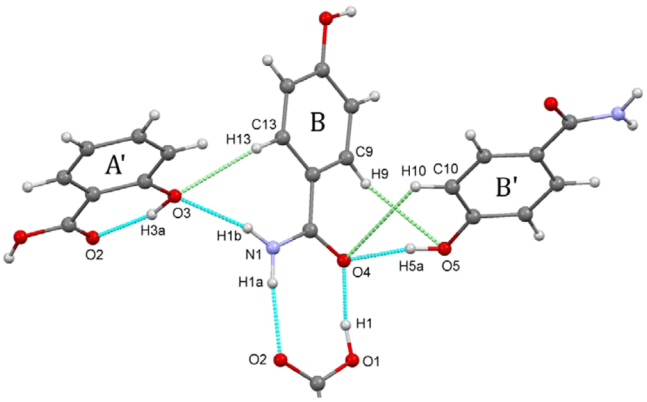

Figure 5. Intermolecular H-bonds and C−H···O contacts between the synthon atoms and O3H3a group of the heterodimer and adjacent molecules in the [SA+4-OHBZA] cocrystal. The part of SA molecule in the dimer is not shown for clarity.

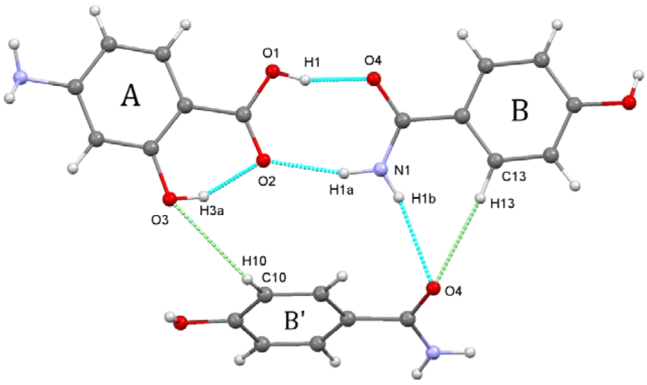

Figure 6. Intermolecular H-bonds and C−H···O contacts between the synthon atoms and O3H3a group of the heterodimer and adjacent molecules in the [PASA+4-OHBZA] cocrystal.

O contacts (Figures 6 and S9−S11). Their energy is below 8 kJ/mol (Table S5). The pattern of calculated intermolecular interactions in [PASA+4-OHBZA] (1:1) is described in Table S5.

The total energy of the secondary interactions formed by the synthon atoms and side hydroxyl group is comparable with that of the acid−amide synthon in [SA+4-OHBZA] (1:1) and [PASA+4-OHBZA] (1:1). In both cocrystals O3 atom has a structure-forming function. It forms several non-covalent bonds with the neighboring molecules, the total energy of these interactions being equal to ∼30 kJ/mol (Tables 4 and 5). Introduction of bulky substituents in the ortho-position to the carbonyl group of salicylates hinders the formation of considered interactions and prevents the formation of 4-OHBZA cocrystals with salicylates such as SSA and ASA. This finding is consistent with the results of our screening (Table S3 and Figures S1−S4).

The cumulative characteristic of non-covalent interactions in solids is the sublimation enthalpy ΔH_{sub}. Its absolute value extrapolated to 0 K corresponds to the crystal lattice energy, E_{latt} (eq 3). The data reported in Table S4 enable us to evaluate ΔH_{sub}(theor) value of the [SA+4-OHBZA] (1:1) cocrystal using eqs 2 and 3. It equals 231 kJ/mol. ΔH_{sub}(theor) is larger than the sum of the absolute sublimation energies of the crystalline SA[49] and 4-OHBZA[50] (∼215 kJ/mol). A similar result has been obtained very recently for the crystalline urea-H_2O_2.[46] The ΔH_{sub}(theor) value of [PASA+4-OHBZA] (1:1) equals 253 kJ/mol. It should be noted that the ΔH_{sub} value remained virtually unchanged when passing from B3LYP/6-31G** to PBE/pob-TZVP (233 vs 231 kJ/mol for [SA+4-OHBZA]; 259 vs 253 kJ/mol for [PASA+4-OHBZA]) (cf. Tables S4 and S6, S5 and S7). According to our computations, the Grimme dispersion correction D2 has practically almost no impact on the theoretical ΔH_{sub} values.

4.4. Solubility and Dissolution Rate Measurements. One of the important advantages of cocrystallization is improving of solubility of poorly soluble drug substances. Therefore, we measured the solubility and IDR of [SA+4-OHBZA] (1:1) and [PASA+4-OHBZA] (1:1) cocrystals in phosphate buffer, pH 7.4. The results of intrinsic dissolution studies and dissolution profiles of the cocrystals and their individual components are shown in Figures 7 and 8.

[SA+4-OHBZA]. Figure 7a shows that the IDR of [SA+4-OHBZA] (1:1) is 1.72 times lower than that of the initial API. Figure 8a shows that the equilibrium solubility of [SA+4-OHBZA] (1:1) is 1.2 times lower than the solubility of SA in pure form and 2 times lower than that of 4-OHBZA. Moreover, there is no "parachute" effect, which is typical of cocrystal dissolution process.[58] Analysis of the bottom phase shows that the cocrystal is stable in solution and does not fall into individual components.

Table 5. Theoretical Values[a] of the D···O and H···O Distances, *R*(D···O) and *R*(H···O), of the D—H···O Fragments (Where D = O, N, or C) and the Electron Density Properties in the H···O Bond Critical Point of the Selected Intermolecular H-Bonds of [PASA+4-OHBZA] (1:1)

interaction	fragment	*R*(D···O), Å (*R*(H···O), Å)	ρ_b, a.u.	$\nabla^2\rho_b$, a.u.	G_b, a.u.	E_{int}[b] kJ·mol^{-1}
		Synthon Interactions				
A···B	O1−H1···O4	2.542 (1.519)	0.071	0.158	0.052	58.5
	N1−H1a···O2	2.884 (1.878)	0.030	0.087	0.022	25.0
					Total:	***83.5***
		Side Interactions of the Synthon Atoms and O3H3a Group[c]				
B···B′	N1−H1b···O4	3.139 (2.153)	0.017	0.046	0.012	13.7
B···B′	C13−H13···O4	3.574 (2.566)	0.007	0.027	0.006	6.5
A···B′	C10−H10···O3	3.371 (2.828)	0.007	0.030	0.006	6.3
A···A′	N2−H2a···O3	3.054 (2.522)	0.009	0.037	0.008	9.0
A···A″	N2−H2b···O3	3.240 (2.557)	0.008	0.030	0.006	7.3
					Total:	***42.8***

[a]Evaluated by solid-state B3LYP/6-31G** followed by Bader analysis of the periodic electronic density. [b]Eq 1. [c]See Figure 6.

DOI: 10.1021/acs.jpcb.5b05082
J. Phys. Chem. B XXXX, XXX, XXX−XXX

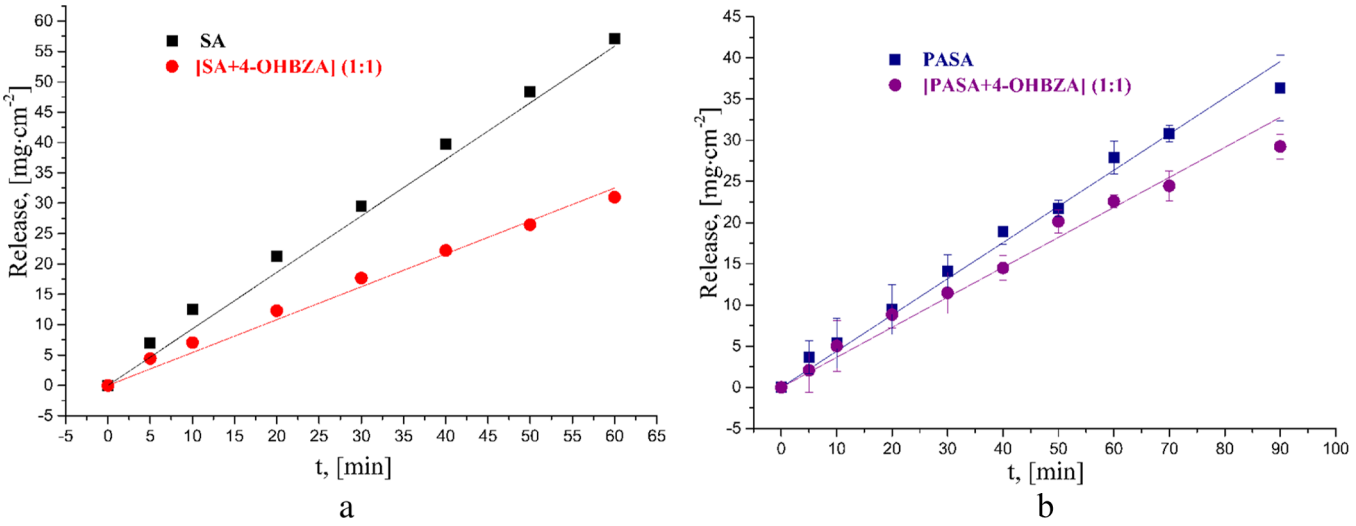

Figure 7. Intrinsic dissolution rates of the cocrystals and APIs in pH 7.4 phosphate buffer at 37.0 °C. The results for PASA and its cocrystal are expressed as mean ± SD, n = 3.

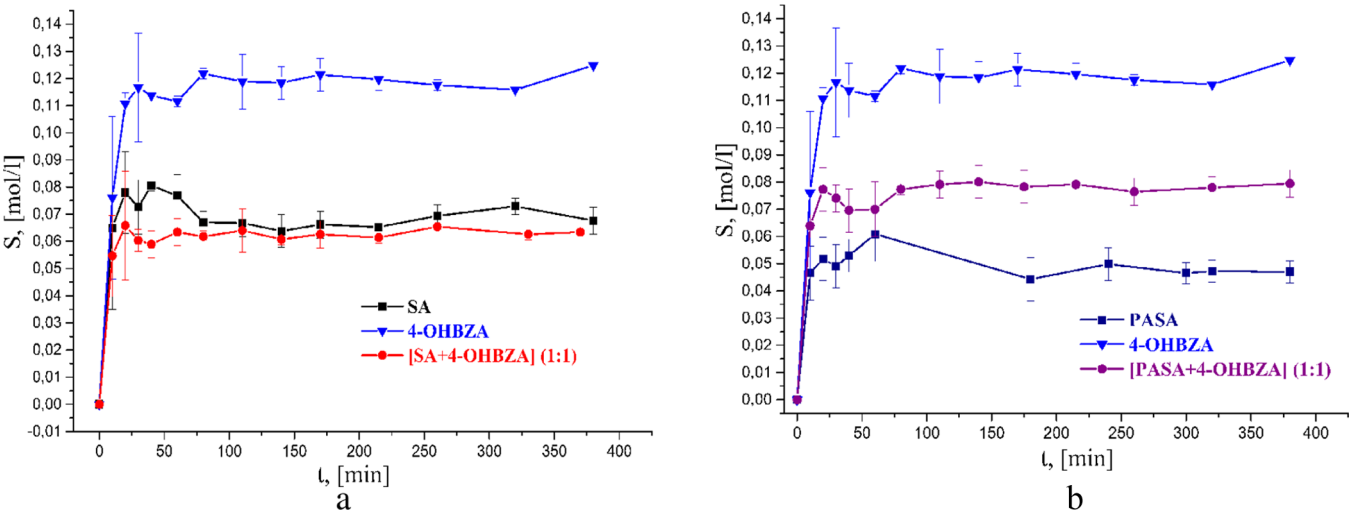

Figure 8. Dissolution profiles for (a) SA, 4-OHBZA, and [SA+4-OHBZA] and (b) PASA, 4-OHBZA, and [PASA+4-OHBZA] in pH 7.4 phosphate buffer at 25.0 °C. The results are expressed as mean ± SD, n = 3.

It is interesting to note that the solubility of the salicylamide cocrystal increased if its value of the crystal lattice energy was close to those of its components.[24] The decrease in the solubility parameter may be explained by the increasing crystal lattice energy value.

[PASA+4-OHBZA]. Figures 7b and 8b represent IDR and solubility curves of [PASA+4-OHBZA] and PASA. The dissolution rate of [PASA+4-OHBZA] is compared to that of pure PASA. The equilibrium solubility of cocrystal is 50% higher than that of PASA. The study of dissolution process of pure PASA by the HPLC method shows the presence of 3-aminophenol in the solution. Figure 9 presents a typical peak at 285 nm in the third minute for 3-aminophenol. The cocrystal solubility study has shown that there is no 3-aminophenol in the solution. Cocrystallization of PASA with 4-OHBZA leads to stabilization of API and blocks its decarboxylation. It is a matter of great importance to find a method for PASA stabilization because 3-aminophenol is a toxic compound. The most commonly employed method to improve physicochemical properties of drug molecules is preparation of inclusion complexes with cyclodextrins.[59] Therefore, obtaining a PASA cocrystal can be considered as an alternative way of API stabilization. The bottom phase analysis of cocrystal dissolution has shown that the para-aminosalicylic acid cocrystal does not fall into individual components in the solution.

5. CONCLUSION

Four derivatives of salicylic acid were chosen for cocrystallization with 4-hydroxybenzamide, based on the heterosynthon approach. Experimental screening produced two new cocrystals, [SA+4-OHBZA] (1:1) and [PASA+4-OHBZA] (1:1). Despite the equal values of calculated acid−amide heterosynthon energy for the four heterodimers, aspirin and salsalate do not form a cocrystal with 4-OHBZA. This shows a crucial role of the secondary interactions in the formation of two-component cocrystals.

To clarify the role of secondary interactions, we performed solid-state DFT computations followed by Bader analysis of the periodic electron density. The total energy of the secondary interactions formed by the synthon atoms and side hydroxyl group was not less than 50% of the energy of heterosynthons for [SA+4-OHBZA] and [PASA+4-OHBZA]. In particular, in

DOI: 10.1021/acs.jpcb.5b05082
J. Phys. Chem. B XXXX, XXX, XXX−XXX

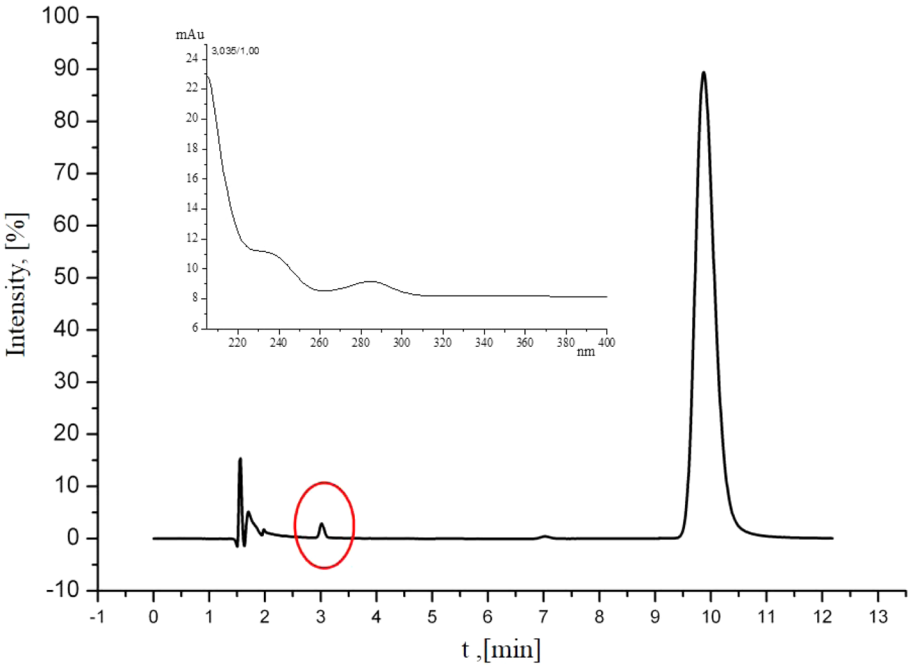

Figure 9. Chromatogram of PASA and 3-aminophenol in water (pH 7.4). Retention times = 3 min for 3-aminophenol and 10 min for PASA. Accuracy of the slope determination is less than 5%.

both cocrystals, the oxygen atom of the ortho-hydroxyl group plays a significant structure-forming role. It forms contacts with the neighboring heterodimers, with the total energy equaling ~30 kJ/mol. Bulky substituents in the ortho-position of salicylates inhibit cocrystal formation of 4-OHBZA with salsalate and aspirin.

Cocrystal [SA+4OHBZA] (1:1) sublimation enthalpy was obtained by the transpiration method. The enthalpy value equals 272 ± 8 kJ/mol, significantly higher than the sum of the sublimation enthalpies of its pure components. The relatively large cocrystal stability in relation to the stability of its components has a negative effect on the dissolution rate and the equilibrium solubility. The [PASA+4-OHBZA] (1:1) cocrystal showed an enhancement of apparent solubility compared to that of the corresponding pure API, while the intrinsic dissolution rates were comparable. Besides that, cocrystal of para-aminosalicylic acid with 4-OHBZA led to increased stability of API to decarboxylation.

■ ASSOCIATED CONTENT

Ⓢ Supporting Information

The Supporting Information is available free of charge on the ACS Publications website at DOI: 10.1021/acs.jpcb.5b05082.

Details of DFT calculations, experimental cocrystal screening results, and thorough hydrogen-bond network topology analysis (PDF)

X-ray crystallographic file for [SA+4-OHBZA] (CIF)

X-ray crystallographic file for [PASA+4-OHBZA] (CIF)

■ AUTHOR INFORMATION

Corresponding Author

*Telephone: +7-4932-533784. Fax: +7-4932- 336237. E-mail glp@isc-ras.ru.

Notes

The authors declare no competing financial interest.

■ ACKNOWLEDGMENTS

This work was supported by the Russian Scientific Foundation (No. 14-13-00640). DSC and PXRD experiments were conducted on the equipment at the center for joint use of scientific equipment, "The Upper Volga Region Center of Physico-Chemical Research".

■ REFERENCES

(1) Stahly, G. P. A Survey of Cocrystals Reported Prior to 2000. *Cryst. Growth Des.* **2009**, *9*, 4212−4229.

(2) Childs, S. L.; Zaworotko, M. J. The Reemergence of Cocrystals: The Crystal Clear Writing is on the Wall Introduction to Virtual Special Issue on Pharmaceutical Cocrystals. *Cryst. Growth Des.* **2009**, *9*, 4208−4211.

(3) Trask, A. V. An Overview of Pharmaceutical Cocrystals as Intellectual Property. *Mol. Pharmaceutics* **2007**, *4* (3), 301−309.

(4) Perlovich, G. L. Thermodynamic Approach to Improving Solubility Prediction of Co-Crystals in Comparison with Individual Poorly Soluble Components. *J. Chem. Thermodyn.* **2014**, *73*, 85−89.

(5) Lu, E.; Rodriguez-Hornedo, N.; Suryanarayanan, R. A Rapid Thermal Method for Cocrystal Screening. *CrystEngComm* **2008**, *10*, 665−668.

(6) Desiraju, G. R. Supramolecular Synthons in Crystal Engineering — A New Organic Synthesis. *Angew. Chem., Int. Ed. Engl.* **1995**, *34*, 2311−2327.

(7) Mukherjee, A.; Desiraju, G. R. Combinatorial Exploration of the Structural Landscape of Acid-Pyridine Cocrystals. *Cryst. Growth Des.* **2014**, *14*, 1375−1385.

(8) Goswami, P. K.; Thaimattam, R.; Ramanan, A. Multiple Crystal Forms of p-Aminosalicylic Acid: Salts, Salt Co-Crystal Hydrate, Co-Crystals, and Co-Crystal Polymorphs. *Cryst. Growth Des.* **2013**, *13* (1), 360−366.

(9) Cherukuvada, S.; Bolla, G.; Sikligar, K.; Nangia, A. 4-Aminosalicylic Acid Adducts. *Cryst. Growth Des.* **2013**, *13*, 1551−1557.

(10) Seaton, C. C.; Parkin, A. Making Benzamide Cocrystals with Benzoic Acids: the Influence of Chemical Structure. *Cryst. Growth Des.* **2011**, *11*, 1502−1511.

DOI: 10.1021/acs.jpcb.5b05082
J. Phys. Chem. B XXXX, XXX, XXX−XXX

(11) Etter, M. C.; MacDonald, J. C.; Bernstein, J. Graph-Set Analysis of Hydrogen-Bond Patterns in Organic Crystals. *Acta Crystallogr., Sect. B: Struct. Sci.* **1990**, *B46*, 256−262.
(12) Bernstein, J.; Davis, R. E.; Shimoni, L.; Chang, N.-L. Patterns in Hydrogen Bonding: Functionality and Graph Set Analysis in Crystals. *Angew. Chem., Int. Ed. Engl.* **1995**, *34*, 1555−1573.
(13) Tothadi, S.; Desiraju, G. R. Synthon Modularity in 4-Hydroxybenzamide−Dicarboxylic Acid Cocrystals. *Cryst. Growth Des.* **2012**, *12*, 6188−6198.
(14) Manin, A. N.; Voronin, A. P.; Drozd, K. V.; Manin, N. G.; Bauer-Brandl, A.; Perlovich, G. L. Cocrystal Screening of Hydroxybenzamides with Benzoic Acid Derivatives: A Comparative Study of Thermal and Solution-Based Methods. *Eur. J. Pharm. Sci.* **2014**, *65*, 56−64.
(15) Lennernäs, H. Regional Intestinal Drug Permeation: Biopharmaceutics and Drug Development. *Eur. J. Pharm. Sci.* **2014**, *57*, 333−341.
(16) WHO. *Expert Committee on Specifications for Pharmaceutical Preparations*, 2006; p 402.
(17) Rainsford, K. D. *Aspirin and Related Drugs*; CRC Press: Boca Raton, FL, 2004; 774 pp.
(18) Grobelny, P.; Mukherjee, A.; Desiraju, G. R. Drug-Drug Co-Crystals: Temperature-Dependent Proton Mobility in the Molecular Complex of Isoniazid with 4-Aminosalicylic Acid. *CrystEngComm* **2011**, *13*, 4358−4364.
(19) Skovsgaard, S.; Bond, A. D. Co-Crystallisation of Benzoic Acid Derivatives with N-Containing Bases in Solution and by Mechanical Grinding: Stoichiometric Variants, Polymorphism and Twinning. *CrystEngComm* **2009**, *11*, 444−453.
(20) McMahon, J. A.; Bis, J. A.; Vishweshwar, P.; Shattock, T. R.; McLaughlin, O. L.; Zaworotko, M. J. Crystal Engineering of the Composition of Pharmaceutical Phases. 3^1. Primary Amide Supramolecular Heterosynthons and Their Role in the Design of Pharmaceutical Co-Crystals. *Z. Kristallogr.* **2005**, *220*, 340−350.
(21) Walsh, R. D. B.; Bradner, M. W.; Fleischman, S.; Morales, L. A.; Moulton, B.; Rodriguez-Hornedo, N.; Zaworotko, M. J. Crystal Engineering of the Composition of Pharmaceutical Phases. *Chem. Commun.* **2003**, 186−187.
(22) Aitipamula, S.; Wong, A. B. H.; Chow, P. S.; Tan, R. B. H. Pharmaceutical Cocrystals of Ethenzamide: Structural, Solubility and Dissolution Studies. *CrystEngComm* **2012**, *14*, 8515−8524.
(23) Lemmerer, A. Covalent Assistance to Supramolecular Synthesis: Modifying the Drug Functionality of the Antituberculosis API Isoniazid *in Situ* During Co-Crystallization with GRAS and API Compounds. *CrystEngComm* **2012**, *14*, 2465−2478.
(24) Manin, A. N.; Voronin, A. P.; Manin, N. G.; Vener, M. V.; Shishkina, A. V.; Lermontov, A. S.; Perlovich, G. L. Salicylamide Cocrystals: Screening, Crystal Structure, Sublimation, Thermodynamics, Dissolution, and Solid-State DFT Calculations. *J. Phys. Chem. B* **2014**, *118*, 6803−6814.
(25) Manin, A. N.; Voronin, A. P.; Perlovich, G. L. Acetamidobenzoic Acid Isomers: Studying Sublimation and Fusion Processes and Their Relation with Crystal Structures. *Thermochim. Acta* **2014**, *583*, 72−77.
(26) Zielenkiewicz, W.; Perlovich, G. L.; Wszelaka-Rylik, M. The Vapour Pressure and the Enthalpy of Sublimation. Determination by Inert Gas Flow Method. *J. Therm. Analys. and Calor.* **1999**, *57*, 225−234.
(27) Dovesi, R.; Orlando, R.; Erba, A.; Zicovich-Wilson, C. M.; Civalleri, B.; Casassa, S.; Maschio, L.; Ferrabone, M.; De La Pierre, M.; D'Arco, P.; et al. CRYSTAL14: A Program for the Ab Initio Investigation of Crystalline Solids. *Int. J. Quantum Chem.* **2014**, *114*, 1287.
(28) Peintinger, M. F.; Oliveira, D. V.; Bredow, T. Consistent Gaussian Basis Sets of Triple-Zeta Valence with Polarization Quality for Solid-State Calculations. *J. Comput. Chem.* **2013**, *34*, 451−459.
(29) Katsyuba, S. A.; Vener, M. V.; Zvereva, E. E.; Fei, Zh.; Scopelliti, R.; Laurenczy, G.; Yan, N.; Paunescu, E.; Dyson, P. J. How Strong is Hydrogen Bonding in Ionic Liquids? Combined X-ray Crystallographic, Infrared/Raman Spectroscopic, and Density Functional Theory Study. *J. Phys. Chem. B* **2013**, *117*, 9094−9105 and references therein.
(30) King, M. D.; Buchanan, W. D.; Korter, T. M. Application of London-Type Dispersion Corrections to the Solid-State Density Functional Theory Simulation of the Terahertz Spectra of Crystalline Pharmaceuticals. *Phys. Chem. Chem. Phys.* **2011**, *13*, 4250−4259 and references therein.
(31) Grimme, S. J. Semiempirical GGA-Type Density Functional Constructed with a Long-Range Dispersion Correction. *J. Comput. Chem.* **2006**, *27*, 1787−1799.
(32) Bader, R. F. W. *Atoms in Molecules—A Quantum Theory*; Oxford University Press: Oxford, 1990.
(33) Tsirelson, V. G. In *Quantum Theory of Atoms in Molecules: from Solid State to DNA and Drug Design*; Matta, C., Boyd, R., Eds.; Wiley-VCH: Weinheim, 2007; Chapter 10.
(34) Gatti, C.; Casassa, S. *TOPOND14 User's Manual*; CNR-ISTM Milano: Milan, Italy, 2014.
(35) Tsirelson, V. G.; Ozerov, R. P. *Electron Density and Bonding in Crystals*; Institute of Physics Publishing: Bristol, England/ Philadelphia, USA, 1996.
(36) Munshi, H.; Guru Row, T. N. Intra- and Intermolecular Interactions in Small Bioactive Molecules: Cooperative Features from Experimental and Theoretical Charge Density Analysis. *Acta Crystallogr., Sect. B: Struct. Sci.* **2006**, *62*, 612−626.
(37) Shishkina, A. V.; Zhurov, V. V.; Stash, A. I.; Vener, M. V.; Pinkerton, A. A.; Tsirelson, V. G. Noncovalent Interactions in Crystalline Picolinic acid N-Oxide: Insights from Experimental and Theoretical Charge Density Analysis. *Cryst. Growth Des.* **2013**, *13*, 816−828.
(38) Mata, I.; Alkorta, I.; Espinosa, E.; Molins, E. Relationships between Interaction Energy, Intermolecular Distance and Electron Density Properties in Hydrogen Bonded Complexes under External Electric Fields. *Chem. Phys. Lett.* **2011**, *507*, 185−189.
(39) Vener, M. V.; Egorova, A. N.; Churakov, A. V.; Tsirelson, V. G. Intermolecular Hydrogen Bond Energies in Crystals Evaluated Using Electron Density: DFT Computations with Periodic Boundary Conditions. *J. Comput. Chem.* **2012**, *33*, 2303−2309.
(40) Vener, M. V.; Shishkina, A. V.; Rykounov, A. A.; Tsirelson, V. G. Cl···Cl Interactions in Molecular Crystals: Insights from the Theoretical Charge Density Analysis. *J. Phys. Chem. A* **2013**, *117*, 8459−8467.
(41) Civalleri, B.; Zicovich-Wilson, C. M.; Valenzano, L.; Ugliengo, P. B3LYP Augmented with an Empirical Dispersion Term (B3LYP-D*) as Applied to Molecular Crystals. *CrystEngComm* **2008**, *10*, 405−410.
(42) Vener, M. V.; Levina, E. O.; Koloskov, O. A.; Rykounov, A. A.; Voronin, A. P.; Tsirelson, V. G. Evaluation of the Lattice Energy of the Two-Component Molecular Crystals using Solid-State DFT. *Cryst. Growth Des.* **2014**, *14*, 4997−5003.
(43) Dominiak, P. M.; Espinosa, E.; Angyan, J. In *Modern Charge Density Analysis*; Gatti, C., Macchi, P., Eds.; Springer: Heidelberg/ London/New York, 2012; pp 387−433.
(44) Gavezzotti, A. Structure and Intermolecular Potentials in Molecular Crystals. *Modell. Simul. Mater. Sci. Eng.* **2002**, *10*, R1−R29.
(45) Day, G. M. Current Approaches to Predicting Molecular Organic Crystal Structures. *Crystallogr. Rev.* **2011**, *17*, 3−52 and references therein.
(46) Medvedev, A. G.; Shishkina, A. V.; Prikhodchenko, P. V.; Lev, O.; Vener, M. V. The Applicability of the Dimeric Heterosynthon Concept to Molecules with Equivalent Binding Sites. A DFT Study of Crystalline Urea-H_2O_2. *RSC Adv.* **2015**, *5*, 29601−29608.
(47) Ouvrard, C.; Mitchell, J. B. O. Can We Predict Lattice Energy from Molecular Structure? *Acta Crystallogr., Sect. B: Struct. Sci.* **2003**, *59*, 676−685.
(48) Luo, Y.-H.; Xu, B.; Sun, B.-W. Investigation of Supramolecular Synthons of p-Hydroxybenzoic Acid (PHBA): Comparison of its Hydrate, Co-Crystal and Salts. *J. Cryst. Growth* **2013**, *374*, 88−98.
(49) Perlovich, G. L.; Volkova, T. V.; Bauer-Brandl, A. Towards an Understanding of the Molecular Mechanism of Solvation of Drug

DOI: 10.1021/acs.jpcb.5b05082
J. Phys. Chem. B XXXX, XXX, XXX−XXX

Molecules: A Thermodynamic Approach by Crystal Lattice Energy, Sublimation, and Solubility Exemplified by Hydroxybenzoic Acids. *J. Pharm. Sci.* **2006**, *95* (7), 1448−1458.
(50) Perlovich, G. L.; Hansen, L. K.; Volkova, T. V.; Mirza, S.; Manin, A. N.; Bauer-Brandl, A. Thermodynamic and Structural Aspects of Hydrated and Unhydrated Phases of 4-Hydroxybenzamide. *Cryst. Growth Des.* **2007**, *7* (12), 2643−2648.
(51) Chikos, J. S.; Acree, W. E. Enthalpies of Sublimation of Organic and Organometallic compounds, 1910−2001. *J. Phys. Chem. Ref. Data* **2002**, *31*, 537−698.
(52) Jivani, S. G.; Stella, V. J. Mechanism of Decarboxylation of p-Aminosalicylic Acid. *J. Pharm. Sci.* **1985**, *74* (12), 1274−1282.
(53) Vetuschi, C.; Ragno, G.; Mazzeo, P. Determination of p-Aminosalicylic Acid and m-Aminophenol by Derivative UV-Spectrophotometry. *J. Pharm. Biomed. Anal.* **1988**, *6* (4), 383−391.
(54) Gatti, C. Chemical Bonding in Crystals: New Directions. *Z. Kristallogr.* **2005**, *220*, 399−457.
(55) Vener, M. V.; Manaev, A. V.; Egorova, A. N.; Tsirelson, V. G. QTAIM Study of Strong H-Bonds with the O-H···A Fragment (A = O, N) in Three-Dimensional Periodical Crystals. *J. Phys. Chem. A* **2007**, *111*, 1155−1162.
(56) Grabowski, S. J. What is the Covalency of Hydrogen Bonding? *Chem. Rev.* **2011**, *111*, 2597−2625.
(57) Vener, M. V.; Egorova, A. N.; Fomin, D. P.; Tsirelson, V. G. Hierarchy of the Non-Covalent Interactions in the Alanine-Based Secondary Structures. DFT Study of the Frequency Shifts and Electron-Density Features. *J. Phys. Org. Chem.* **2009**, *22*, 177−185.
(58) Babu, N. J.; Nangia, A. Solubility Advantage of Amorphous Drugs and Pharmaceutical Cocrystals. *Cryst. Growth Des.* **2011**, *11* (7), 2662−2679.
(59) Roik, N. V.; Belyakova, L. A. Cyclodextrin-Based Drug Stabilizing System. *J. Mol. Struct.* **2011**, *987*, 225−231.

DOI: 10.1021/acs.jpcb.5b05082
J. Phys. Chem. B XXXX, XXX, XXX−XXX